Global Change Biology

Global Change Biology (2015) **21**, 2022–2039, doi: 10.1111/gcb.12817

Measured and modeled interactive effects of potassium deficiency and water deficit on gross primary productivity and light-use efficiency in *Eucalyptus grandis* plantations

MATHIAS CHRISTINA[1,2], GUERRIC LE MAIRE[1], PATRICIA BATTIE-LACLAU[3], YANN NOUVELLON[1,4], JEAN-PIERRE BOUILLET[1,5], CHRISTOPHE JOURDAN[1], JOSÉ LEONARDO DE MORAES GONÇALVES[5] and JEAN-PAUL LACLAU[1,5,6]

[1]*UMR Eco&Sols, CIRAD, 2 place Viala, 34060 Montpellier, France,* [2]*SupAgro Montpellier, 2 place Viala, 34060, Montpellier, France,* [3]*CENA, Universidade de São Paulo, 13400-970 Piracicaba, SP, Brazil,* [4]*Departamento de Ciencias Atmosfericas, Universidade de São Paulo, 05508-900 São Paulo, SP, Brazil,* [5]*ESALQ, Universidade de São Paulo, 13400-970 Piracicaba, SP, Brazil,* [6]*Forest Science Department, UNESP, 18610-307 Botucatu, SP,Brazil*

Abstract

Global climate change is expected to increase the length of drought periods in many tropical regions. Although large amounts of potassium (K) are applied in tropical crops and planted forests, little is known about the interaction between K nutrition and water deficit on the physiological mechanisms governing plant growth. A process-based model (MAESPA) parameterized in a split-plot experiment in Brazil was used to gain insight into the combined effects of K deficiency and water deficit on absorbed radiation (aPAR), gross primary productivity (GPP), and light-use efficiency for carbon assimilation and stem biomass production (LUE_C and LUE_s) in *Eucalyptus grandis* plantations. The main-plot factor was the water supply (undisturbed rainfall vs. 37% of throughfall excluded) and the subplot factor was the K supply (with or without 0.45 mol K m^{-2} K addition). Mean GPP was 28% lower without K addition over the first 3 years after planting whether throughfall was partly excluded or not. K deficiency reduced aPAR by 20% and LUE_C by 10% over the whole period of growth. With K addition, throughfall exclusion decreased GPP by 25%, resulting from a 21% decrease in LUE_C at the end of the study period. The effect of the combination of K deficiency and water deficit was less severe than the sum of the effects of K deficiency and water deficit individually, leading to a reduction in stem biomass production, gross primary productivity and LUE similar to K deficiency on its own. The modeling approach showed that K nutrition and water deficit influenced absorbed radiation essentially through changes in leaf area index and tree height. The changes in gross primary productivity and light-use efficiency were, however, driven by a more complex set of tree parameters, especially those controlling water uptake by roots and leaf photosynthetic capacities.

Keywords: carbon assimilation, eucalypt, fertilization, modeling, nutrient shortage, radiation-use efficiency, tree traits

Received 1 September 2014 and accepted 6 October 2014

Introduction

Global climate change will result in rising average temperatures and more frequent droughts in many regions (Seager *et al.*, 2007; Sheffield & Wood, 2008; IPCC, 2013). How future rainfall distribution will alter carbon (C), water and nutrient cycling has therefore broad implications for tropical forests. Recent studies highlighted the need to gain insight into the effects of global climate change on tree nutrition and the consequences on forest ecology (Kreuzwieser & Gessler, 2010; Peñuelas *et al.*, 2013; Piao *et al.*, 2013). In highly productive planted forests, tree grow is largely dependent on fertilization regimes (e.g. Smethurst, 2010; Gonçalves *et al.*, 2013). Planted forests provided 39% of the global wood consumption in 2010 (FAO, 2011), and their contribution to satisfying the global wood demand should increase in the future (Paquette & Messier, 2010).

Management practices can help to mitigate the adverse consequences of drought in planted forests (White *et al.*, 2009). In particular, the beneficial effects of an adequate nutritional status on plant resistance to abiotic stresses are well established (Reddy *et al.*, 2004). Potassium (K) nutrition influences plant growth in dry environments through the strong effects of foliar K on leaf osmotic adjustment (Mengel & Arneke, 1982; Battie-Laclau *et al.*, 2014a), stomatal regulation (Cochrane & Cochrane, 2009; Battie-Laclau *et al.*, 2014a,b), protection against oxidative damage (Cakmak, 2005; Wang *et al.*, 2013) and photosynthate loading into the phloem sap (Cakmak *et al.*, 1994; Gajdanowicz *et al.*, 2011). However, despite the beneficial effects of K nutrition

Correspondence: Mathias Christina, tel. +33(0)665400582, fax 33(0)499612119, e-mail: mathias.christina@cirad.fr

on leaf water relations, a recent study of *Eucalyptus grandis* plantations showed that the increase in tree water demand in response to K supply reduced water storage in deep soil layers during rainy periods, which led to an increase in water deficit during severe droughts (Battie-Laclau *et al*., 2014b). Although K nutrition has been much less studied than nitrogen and phosphorus nutrition in forest ecosystems, recent studies showed that gross primary productivity (GPP) is strongly K-limited over large tropical areas (Römheld & Kirkby, 2010; Darunsontaya *et al*., 2012; Santiago *et al*., 2012; Gonçalves *et al*., 2013). A wide range of morphological and physiological traits are modified by the K and water supply regimes (Zhang, 1996; Egilla *et al*., 2001; Laclau *et al*., 2009). A modeling approach is therefore needed to assess the contribution of each traits to plant C assimilation and tree growth because experimental approaches cannot disentangle the effects of interacting plant adaptations. So far as we are aware, process-based models have not been used to gain insight into the main tree parameters (morphological, physiological and root) driving GPP and light-use efficiency under different K and water supply regimes in tropical forests.

The Earth's GPP results from the capacity of plants to absorb photosynthetically active radiation (PAR) and to use this absorbed photosynthetically active radiation (aPAR) to synthesize carbohydrates through photosynthesis. Light-use efficiency for C assimilation (LUE_C, the ratio between GPP and aPAR) is commonly used to estimate GPP from remote sensing data (e.g. Yang *et al*., 2007; Hilker *et al*., 2008; Sjöström *et al*., 2013). Light-use efficiency for stem biomass production (LUE_S, the ratio between the increase in stem biomass and aPAR) is also widely used in studies dealing with forest management (Binkley *et al*., 2013; Le Maire *et al*., 2013). Binkley *et al*. (2004, 2010) showed that, in tropical planted forests, LUE_S generally increases with the availability of water and nitrogen. Nevertheless, the effect of K nutrition on tree parameters driving LUE has never been studied for forest ecosystems.

A better understanding of the effects of nutrients, water supply and their interactions on tree functioning is required for the management of planted forests in a changing climate. A process-based model (MAESPA, Duursma & Medlyn, 2012) was used to investigate the main tree parameters accounting for the changes in aPAR, LUE and GPP under different K and water supply regimes in *Eucalyptus* plantations. These planted forests cover about 20 million hectares throughout the world and are expanding rapidly in tropical and subtropical regions (Booth, 2013). We hypothesized that (i) K deficiency and water deficit lead to a decrease in GPP resulting from a decrease in both aPAR and LUE, (ii) a modeling approach using the MAESPA model makes it possible to assess the contribution of each tree trait to GPP and LUE, under different K and water supply regimes, and (iii) the effects of K deficiency and water deficit are nonadditive and the interaction between them strongly influences aPAR, LUE and GPP.

Materials and methods

Site description

The experiment was conducted at the Itatinga Experimental Station of the University of São Paulo in Brazil (23°02′S; 48°38′W). Over the last 15 years, the mean annual rainfall was 1360 mm and the mean annual temperature was 20°C. The dry season was from June to September with a mean monthly temperature of 15°C, and the rainy season was from October to May, with a mean monthly temperature of 25°C and higher overall PAR. The experiment was located on a hilltop (slope <3%) at an altitude of 850 m. The soils were very deep Ferralsols (>15 m; Christina *et al*., 2011) developed on Cretaceous sandstone, with clay content ranging from 14% in the top soil to 23% in deep soil layers and mean concentrations of exchangeable K of 0.02 $cmol_c\ kg^{-1}$ in the upper soil layer and <0.01 $cmol_c\ kg^{-1}$ at a depth of 5–1500 cm (Laclau *et al*., 2010).

Experimental design

A split-plot experimental design was set up in June 2010 with a highly productive *E. grandis* clone used in commercial plantations by the Suzano Company (São Paulo, Brazil). The experiment was described in detail by Battie-Laclau *et al*. (2014b). Four treatments (two fertilization regimes × two water supply regimes) were applied in three blocks. The area of individual plots was 864 m^2 (144 trees per plot). The main-plot factor was the water supply regime (approximately 37% throughfall exclusion, −W, vs. no throughfall exclusion, +W) and the subplot factor was the fertilization regime (with 0.45 mol K m^{-2} applied as KCl, +K vs. no K addition, −K). The K was applied 3 months after planting and provided nonlimiting K availability for tree growth (Almeida *et al*., 2010). The treatments were as follows:

+K+W: K addition and no throughfall exclusion, the reference for comparisons;
−K+W: no K addition and no throughfall exclusion;
+K−W: K addition with throughfall exclusion;
−K−W: no K addition with throughfall exclusion.

Other nutrients were applied at planting for all treatments (3.3 g P m^{-2}, 200 g m^{-2} of dolomitic lime and trace elements) and at 3 months (12 g N m^{-2}), which was nonlimiting for tree growth at this study site (Laclau *et al*., 2009). Throughfall was excluded using panels made of clear, PAR-transmitting greenhouse plastic sheets mounted on wooden frames at a height of 1.6–0.5 m.

MAESPA model

The MAESPA model (Duursma & Medlyn, 2012) coupled the soil water balance components of the SPA model (Williams *et al.*, 2001a,b) to the MAESTRA model (Wang & Jarvis, 1990a; Medlyn *et al.*, 2007), with some major changes and additions. The MAESTRA model had a long history of development and application to diverse forest types (http://maespa.github.io/bibliography.html). MAESTRA was a 3D single-tree and stand process-based model that calculated light interception and distribution within crowns, and used a leaf physiology submodel to estimate photosynthesis and transpiration. The three-dimensional model for calculating aPAR was based on Norman & Welles (1983) and is described in other studies (e.g. Wang & Jarvis, 1990b; Medlyn, 1998; Bauerle *et al.*, 2004). The spatial position, crown dimensions and total leaf area of each tree of the stand were inputs to the model. aPAR was calculated for specified 'target' trees of the stand, taking into account neighboring trees competing for light. The crown was discretized in a 3D grid point with a given number of horizontal layers and a given number of points per layer. For each point of the grid, the leaf area density and the leaves inclination distributions were calculated using normalized beta-distributions. At each grid point, both photosynthesis and transpiration were calculated using a combined stomatal conductance/photosynthesis/transpiration model based on Farquhar *et al.* (1980) for CO_2 assimilation and Tuzet *et al.* (2003) for stomatal conductance. The water balance submodel was largely derived from SPA routines (Williams *et al.*, 2001a,b). The soil profile comprised various horizontally uniform soil layers with specific characteristics and root densities. The water storage in each soil layer was calculated from the infiltration, drainage, root water uptake and soil evaporation at the same time-step as the aboveground processes (half-hourly in general).

Meteorological data

Meteorological data were obtained from June 2010 to June 2013 using an automatic station placed on the top of a 21-m tower located 50 m from the experiment. Half-hourly meteorological inputs were incident PAR (μmol m^{-2} s^{-1}), air temperature (°C), relative humidity (%), atmospheric pressure (Pa), wind speed above the canopy (m s^{-1}) and precipitation (mm).

Canopy structure parameters

Tree position, crown dimensions, leaf area and stem biomass. The XY coordinates of each tree within the plot were specified in MAESPA, as well as the position of the plot relative to the north and east (Fig. 1). The tree height, crown length and radius, and leaf area of each tree were calculated based on inventories carried out in each plot monthly from 6 to 17 months after planting and then at ages 23, 27, 31 and 36 months. The tree size parameters were estimated by linear interpolation between each inventory. The crown diameter (D_c) was measured along the planting row and across the row up to 10 months. Thereafter, the tree height (H) and trunk circumference at breast height (CBH) were measured and D_c was estimated using the allometric relationship ($D_c = a \times \log(H)^b$), where a and b are fitted parameters. The tree leaf area (LA) was measured destructively for eight trees for each treatment at 8 (six trees only), 11, 16, 23, 28 and 36 months after planting. When the trees were felled, the crown was divided into three crown sections of equal length, and the leaf area in each of these crown sections was calculated from the leaf biomass and specific leaf area measurements. The tree leaf area was then calculated by summing the leaf area of the three crown sections. Age-specific allometric relationships between LA and the tree size were determined for each treatment and then applied to estimate LA for all the trees in the plots for each treatment using inventory data. Two allometric relationships were used: LA was predicted either using $c(D_cH)^d$ up to 11 months, or using $e(CBH^2H)^f$ thereafter, where c, d, e and f are fitted parameters. The relationships for the different ages were tested using Akaike (AIC) and Bayesian (BIC) information criteria. Allometric relationships were determined for the crown length and for the crown radius along the row and across the row. Treatment- and age-specific allometric relationships ($g + h(CBH^2H)^i$) were established at 12, 24 and

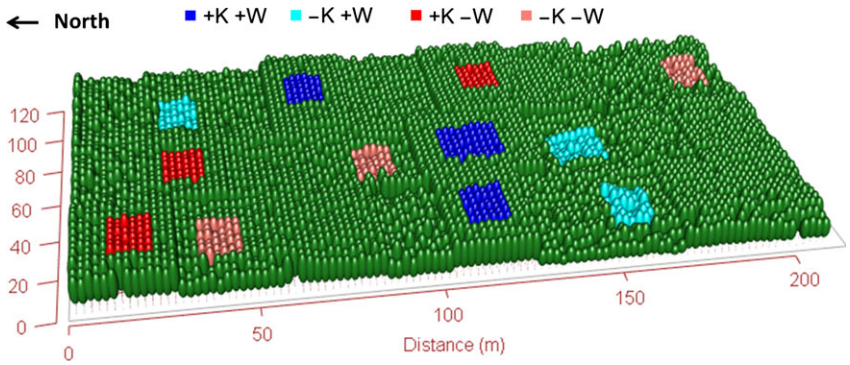

Fig. 1 Plot design used in MAESPA simulations. The four treatments were potassium fertilization (+K) vs. potassium deficiency (−K) crossed with undisturbed rainfall (+W) vs. exclusion of 37% of throughfall (−W). Central trees within each plot are shown in dark blue for +K+W, in red for +K−W, in light blue for −K+W and in pink for −K−W. Border trees are shown in green.

36 months to estimate the stem biomass for all the trees in the experiment. The stem carbon (C) contents in the stem biomass were estimated assuming that 1-kg stem dry matter was equal to 0.47 kgC, as measured in *E. grandis* trees at the same age in a nearby plantation (Nouvellon *et al*., 2012). Finally, the crown shape was assumed to be half-ellipsoid for all trees. Border trees surrounding each plot were included in the simulations with their true position and size (dark green trees in Fig. 1), to take into account competition for light between the different plots. Details of the variable names, definitions and units are given in Table 1.

Leaf angle distribution. The leaf inclination angle distributions (LIA) were measured at 12, 24 and 36 months for eight trees in each treatment over the range of tree sizes. Twelve auxiliary branches (four for each of the upper, middle and lower crown sections, at four azimuth angles) representative of the crown were selected in each tree. The leaf inclination angles were measured with a digital clinometer on six leaves per branch (72 leaves per tree). The leaf area distribution in nine inclination angle classes (from 0 to 90°) was calculated and used as input in MAESPA for radiative transfer.

Vertical and horizontal leaf area distribution within the tree crown. The MAESPA model distributes the leaf area within the tree crown using the product of two beta functions (for vertical and horizontal leaf area distributions). The parameters of the beta function used for the vertical distribution were estimated using the leaf areas measured in the three crown sections of each tree destructively sampled (see 'tree position, crown dimensions, leaf area and stem biomass' above). The horizontal beta-distribution was computed for eight trees in each treatment at 12 and 24 months. The distance between the trunk and the leaves was measured on all branches in each third of the crown height. The number of leaves, used as a proxy for the leaf area (there was little variation in leaf size from the interior to the periphery of the crown), was plotted as a function of the distance from the trunk, allowing the beta function for the horizontal distribution to be adjusted. Horizontal beta-distributions were combined for tree ages and treatments using AIC and BIC (Table S1).

Plant physiological parameters

Photosynthetic parameters. The quantum yield (α, mol e^- mol^{-1} aPAR) and the curvature of the light response of the electron transportation curve (θ, dimensionless) were estimated at 2 years using light response curves obtained for leaves in three vertical positions within the crown (lower, medium and upper third of the crown) for three trees in each treatment. Measurements were made using a portable gas exchange system (LI-COR 6400; LI-COR Inc., Lincoln, NE, USA) at constant CO_2 concentration (380 ppm). Each measurement was initiated at PAR = 1500 μmol m^{-2} s^{-1}, and subsequent photosynthesis measurements were made at PAR = 2000, 1500, 1000, 750, 500, 250, 125, 63, 32 and

Table 1 List of symbols, definitions and units of variables used in the model and discussed within the paper

Variable	Definition	Unit
LAI	Leaf area index	m^2 m^{-2}
LA	Tree leaf area	m^2
H	Tree height	m
CBH	Trunk circumference at breast height	m
D_c	Crown diameter	m
LIA	Mean leaf inclination angle	°
LAD	Leaf area density	Dimensionless
J_{MAX}	Maximum rate of photosynthetic electron transport at 25°C	μmol m^{-2} s^{-1}
V_{CMAX}	Maximum rate of Rubisco carboxylase activity at 25°C	μmol m^{-2} s^{-1}
R_d	Dark respiration at 25°C	μmol m^{-2} s^{-1}
θ	Curvature of the light response of electron transportation curve	Dimensionless
α	Quantum Yield	mol e^- mol^{-1} aPAR
W_{leaf}	Leaf width	m
RMD	Fine root mass density	g m^{-2}
RAD	Root radius	mm
SRL	Specific root length	m g^{-1}
R_{dis}	Root mass distribution	Dimensionless
K_p	Leaf-specific total plant conductivity	mmol m^{-2} s^{-1} MPa^{-1}
θ_M	Minimum volumetric soil water content	m^3 m^{-3}
aPAR	Absorbed photosynthetically active radiation	MJ m^{-2} day^{-1}
GPP	Gross primary productivity	gC m^{-2} day^{-1}
LUE_S	Light-use efficiency for stem biomass production	gDM MJ^{-1}
LUE_C	Light-use efficiency for C assimilation	gC MJ^{-1}
%GPPstem	Fraction of assimilated C allocated to stem wood production	gC gC^{-1}
Δ_{stem}	Stem biomass increment	kgDM $tree^{-1}$ yr^{-1}

0 μmol m^{-2} s^{-1}, after stomatal conductance equilibrium. The Farquhar model (Farquhar *et al.*, 1980; Medlyn *et al.*, 2002) was used to fit α and θ.

A–Ci curves were measured using the LI-COR 6400 at three vertical positions and two horizontal positions within the crown (inner and outer leaves) for three trees per treatment, at 20 and 32 months of age (total of 144 A–Ci curves for each age). Measurements were made at various CO_2 concentrations (400, 300, 250, 200, 150, 100, 75, 50 ppm and then 400, 600, 800, 1000, 1300 ppm) at constant PAR (1600 μmol m^{-2} s^{-1}). Photosynthetic parameters J_{MAX}, V_{CMAX} and dark respiration (R_d) at 25°C were fitted simultaneously to the Farquhar model (according to Miao *et al.*, 2009), using the Nelder & Mead (1965) method. 500 random initial parameters were simulated for each curve and the best fit under the RMSE criteria was selected. These parameters were included in MAESPA as a function of the height within the crown for each treatment (Fig. S1).

Stomatal conductance parameters. Photosynthesis, stomatal conductance and leaf water potential were measured monthly from 16 to 36 months (data set from Battie-Laclau *et al.*, 2014b). MAESPA parameters were obtained by fitting the Tuzet *et al.* (2003) model using the Nelder & Mead (1965) method:

$$g_s = g_0 + g_1 \times \frac{A_n}{C_s - \gamma} \times f(\Psi_L) \quad (1)$$

where A_n is the leaf net assimilation rate (μmol m^{-2} s^{-1}), g_0 is the conductance when A_n is zero, g_1 is an empirical parameter, C_s is the CO_2 concentration at the leaf surface (μmol mol^{-1}), γ is the CO_2 compensation point, and $f(\Psi_L)$ is a function of response of stomatal conductance to vapor pressure deficit and soil water deficit controlled by the leaf water potential (Ψ_L, MPa)

$$f(\Psi_L) = \frac{1 + \exp(S_f \Psi_f)}{1 + \exp[s_f(\Psi_f - \Psi_L)]} \quad (2)$$

where S_f and Ψ_f are parameters, Ψ_f is a reference water potential (MPa), and S_f is the 'steepness' of the response of $f(\Psi_L)$ to Ψ_L. AIC and BIC showed that the parameters were identical for all treatments (Table S2, $g_0 = 0.01$, $g_1 = 18.7$, $\gamma = 0.12$, $S_f = 0.49$ and $\Psi_f = -1.99$). The leaf width, which was an input parameter for MAESPA used for leaf boundary layer calculations, was measured on 20 upper leaves of four trees in each treatment (method described by Battie-Laclau *et al.*, 2013) at 24 months and did not change between treatments.

Plant hydraulic conductivity. The whole-plant hydraulic conductivity (K_p) was estimated from sap flow measurements and from the water potential gradient from roots to leaves at midday measured every 1–2 months from 16 to 36 months. The sap flow and leaf water potential were measured on four trees for each treatment. The average tree transpiration between 12:00 and 14:00 per unit leaf area was divided by the difference between the predawn and midday leaf water potentials, to obtain the whole-tree leaf-specific conductivity (for details see Carter & White, 2009).

Soil characteristics and root parameters

Soil characteristics. The soil profiles were divided into layers down to a depth of 13.5 m to take into account the variability of soil and root characteristics depending on soil depth: 0–20, 20–50 cm, four layers 50 cm thick and 11 layers 1 m thick down to 13.5 m. The soil retention curves (Van Genuchten, 1980) and hydraulic conductivity were estimated using a data set obtained by Maquere (2008) at the same site. The residual soil water content (θ_M) in each soil layer was forced in MAESPA to reach the minimum soil water content values measured in each treatment down to 10 m depth (no drainage or water uptake). The soil hydraulic conductivity (K_{sat}) was measured at the same site down to a depth of 3 m (Maquere, 2008) and was assumed to be constant for deeper soil layers (there was little change in particle size fractions).

Root parameters. The root distribution (R_{dis}), root radius (RAD), specific root length (SRL) and total fine root mass (RMD) were measured at 12, 24 and 36 months by soil coring (as described in Christina *et al.*, 2011) in each treatment down to a depth of 13 m. The root parameters in MAESPA were treatment-specific over the study period. At 12 months, the fine root biomass was measured down to 2 m depth in all treatments and fine root biomass from 2 to 6 m was estimated using the distribution found by Christina *et al.* (2011) in a nearby stand. The root distribution was linearly interpolated in MAESPA between measurement dates.

Validation of canopy gap fractions

The directional gap fractions (GFs) were measured with a LI-COR PCA LAI-2000 (LiCor, Lincoln, NE, USA) at five dates between 2 and 3 years in all treatments in block 1 (one plot per treatment). In each plot, 12 measurements were taken below the canopy following the standard protocol described by Le Maire *et al.* (2013). Using MAESPA, the GFs were predicted at the same locations and on the same dates as the measurements were taken. For these predictions, the leaf reflectance and transmittance were set to values close to 0 because the optical filter of the LAI-2000 detects light in a part of the spectrum where leaf reflectance and transmittance are very low (LAI-2000 manual). The simulated and measured directional GFs were averaged for each treatment and compared.

Simulations, statistical and output analyses

Statistical analyses. The effects of the W and K supply regimes on the tree leaf area (LA), tree height (H), crown diameter (D_c), leaf angle (LIA), root-to-leaf conductivity (K_p), photosynthetic parameters (J_{MAX}, V_{CMAX}, R_d, θ and α), leaf width (W_{leaf}), root biomass density (RMD), radius (RAD) and specific root length (SRL) were tested using a linear mixed model. The W and K supply regimes as well as the tree age were considered to be fixed effects and the blocks, and the interactions between W and blocks were considered as random effects (Table 2). The effects of W and K regimes as well

Table 2 Effects of throughfall exclusion (W) and potassium (K) fertilization regimes, tree age and their interaction on 14 parameters described in Table 1

	W	K	Age	W × K	W × Age	K × Age	W × K × Age
Morphological parameters							
LA	ns	***	***	ns	***	***	***
H	*	***	***	***	***	***	***
D_c	*	***	***	**	***	***	**
LIA	*	***	***	ns	***	***	ns
Physiological parameters							
J_{MAX}	ns	***	ns	*	*	ns	ns
V_{CMAX}	ns	***	***	ns	***	ns	ns
R_d	***	***	***	ns	ns	ns	ns
θ	ns	ns		ns			
α	ns	ns		*			
W_{leaf}	ns	ns		ns			
K_p	ns	ns	***	ns	ns	ns	*
Root parameters							
RMD	ns	ns	**	*	ns	ns	ns
RAD	ns	**	***	ns	*	ns	ns
SRL	ns	*	***	ns	ns	ns	*

Block and W*block were used as random effects in the mixed linear model.
*, ** and *** show significant differences at $P < 0.05$, <0.01 and <0.001, respectively; ns indicates no significant differences.

as tree age on the allometric relationships for vertical and horizontal leaf area distributions and stomatal conductance models were assessed using AIC and BIC (Table S2). When the effects of W, K, age and their interactions on parameters were not significant, mean values were fixed in the MAESPA model. Statistical analyses were performed with R 4.0 (R Development Core Team, 2014, package nlme, gss, 2013).

Simulations and output analyses. A complete model representing the 4254 trees in the experiment was built using MAESPA (Fig. 1). Simulations for the 36 inner trees in each subplot were performed over 3 years at half-hourly time steps, for the four treatments and the three blocks. The daily GPP and daily aPAR were estimated for each tree, totaled for the entire inner subplot and then divided by the area to give a stand-scale GPP (gC m^{-2} day^{-1}). The light-use efficiency for carbon assimilation (LUE_C, gC MJ^{-1}) was obtained by dividing the simulated stand GPP by the simulated stand aPAR (MJ m^{-2} day^{-1}). The light-use efficiency for stem biomass production (LUE_S, kgDM MJ^{-1}) was obtained for each tree by dividing the measured tree stem biomass increment (Δ_{stem}, kgDM yr^{-1} $tree^{-1}$) by the tree aPAR (MJ yr^{-1} $tree^{-1}$). The proportion of assimilated C allocated to the stem ($\%GPP_{stem}$) was obtained by dividing the measured tree stem biomass increment (gC yr^{-1} $tree^{-1}$) by the simulated tree gross photosynthesis (gC yr^{-1} $tree^{-1}$). For a better visual interpretation, daily changes in aPAR, GPP and LUE_C were fitted using smoothing spline functions with Gaussian regression (Kim & Gu, 2004).

Analysis of individual and combined effects. The individual effects of K deficiency and W deficit and their combined effect on the measured stem biomass production, simulated aPAR, GPP and LUE_C were calculated annually using the method proposed by Luo *et al.* (2008). For example, in the case of aPAR, the effect of K deficiency (Eff_K), W deficit (Eff_W) and the combined K and W effects (Eff_{KW}) were as follows:

$$Eff_K = aPAR_{-K+W} - aPAR_{+K+W} \quad (3)$$

$$Eff_W = aPAR_{+K-W} - aPAR_{+K+W} \quad (4)$$

$$Eff_{KW} = aPAR_{-K-W} - aPAR_{+K+W} \quad (5)$$

The interaction between K deficiency and W deficit (Int) was calculated as the difference between the combined effect of K and W (Eff_{KW}) and the sum of the effects of K and W individually (Eff_K + Eff_W). Changes in stem biomass production were measured annually during the experiment, and changes in aPAR, GPP and LUE_C with K deficiency and W deficit relative to the +K+W treatment (used as the reference treatment in this study) were calculated annually from MAESPA simulations.

Hierarchy between tree parameters. The consequences of tree parameters affected by K deficiency and W deficit on aPAR, GPP and LUE_C the third year after planting were calculated using the same sensitivity method as Luo *et al.* (2008). aPAR, GPP and LUE were compared during the third year after planting (between months 24 and 36), corresponding to the period with the highest tree response to K deficiency and W deficit.

The first-order effect of a given tree parameter affected by K deficiency (for a given W deficit) was tested by comparing simulated aPAR, GPP and LUE_C in +K+W, with simulations

in the same +K+W treatment with the target tree parameter forced to the value observed for the −K+W treatment. The same procedure was used for parameters affected by W deficit. For instance, the effect of parameter i measured in the −K+W treatment (Effp_i) on aPAR in response to K deficiency was computed as follows:

$$\mathrm{Eff}p_i = \mathrm{aPAR}_{+\mathrm{K}+\mathrm{W},i1} - \mathrm{aPAR}_{+\mathrm{K}+\mathrm{W},i0} \quad (6)$$

where i_1 and i_0 are the values of parameter i in treatments +K+W and −K+W, respectively. The tree parameters studied were leaf area index (LAI), tree height (H), tree crown diameter (D_c), leaf inclination angle (LIA), leaf area density (LAD), J_{MAX}, V_{CMAX}, R_d, quantum yield for electron transport (α), leaf-specific total plant conductance (K_p), total root biomass (RMD), root radius (RAD), specific root length (SRL), root biomass distribution (R_{dis}) as well as the minimum soil water content (θ_M) in each layer and the W supply regime (*Rain*) taken into account in the model.

Although it is difficult to calculate the interaction between two or more tree parameters, the overall interaction between all the parameters affected by K or W limitation could be estimated as the difference between the results of simulations substituting simultaneously all the parameters in the +K+W treatment by their value in the treatment under K or W limitation and the sum of the main effects of all the parameters substituted 1 by 1 in the +K+W treatment. For instance, the interaction between the n tree parameters affected by K deficiency (Int$_p$) on aPAR, was as follows:

$$\mathrm{Int}_p = \left(\mathrm{aPAR}_{-\mathrm{K}+\mathrm{W}} - \mathrm{aPAR}_{+\mathrm{K}+\mathrm{W}}\right) - \sum_{i=1}^{n} \mathrm{Eff}p_i \quad (7)$$

Results

Effects of potassium and water deficiencies on tree parameters

Throughfall exclusion as well as K deficiency changed the tree morphology considerably (Tables 2 and 3). At 3 years, the mean LAI, H, D_c and LIA of K-deficient trees were 64%, 45%, 0% and 15% lower, respectively, than trees with added K in +W, and 53%, 30%, 5% and 15% lower in −W (Table 3). K addition changed the vertical LAD, with a higher proportion of leaves at the bottom of the crown in K-deficient trees than in trees with added K (Table S2). However, the horizontal LAD was not affected by K addition. Exclusion of 37% of throughfall led to a significant decrease in H, D_c as well as LA, but only in +K and at the end of the study period. Throughfall exclusion did not affect LAD for either K treatment. The water supply regime had a significant effect on leaf area, tree height, crown diameter and leaf angle, depending on tree age.

The K and W supply regimes significantly affected the main parameters driving leaf photosynthetic capacity (Table 2). At 3 years, J_{MAX}, V_{CMAX} and R_d in K-deficient trees were 21%, 31% and 9% lower, respectively, than in trees with added K in +W, and 7%, 29% and 23% lower in −W (Table 3). θ was not affected by the W and K supply regimes and averaged 0.69. The W deficit was significant depending on tree age for J_{MAX} and V_{CMAX}, as a result of a strong decrease in J_{MAX} and V_{CMAX} in response to throughfall exclusion that only occurred at the end of the study period (Table 3). K_p was 27% lower in K-deficient trees across the two W supply regimes during the second year of growth. Throughfall exclusion led to a 27% increase in K_p in the third year for both K supply regimes (Tables 2 and 3). The relationship between stomatal conductance and photosynthesis (Tuzet *et al.*, 2003 model, eqns 1 and 2) was similar for all treatments (Table S2).

The root parameters were strongly influenced by the K and W supply regimes (Tables 2 and 3). The fine root biomass at 3 years ranged from 598 to 960 g m^{-2}. It was 23% lower in K-deficient trees in +W and 38% lower in −W. The mean root radius increased significantly with tree age, and K deficiency led to a RAD 13% lower in −K than in +K, for both W supply regimes (Table 3). SRL decreased with tree age and was 10% higher in −K than in +K for both W supply regimes. The minimum soil water content (θ_M) was strongly affected by the K and W supply regimes. The mean θ_M across the soil layers explored by fine roots over the study period was 15% lower in +K−W and 4% higher in −K+W (Table 3). However, K addition did not affect θ_M in the −W plots. θ_M linearly increased with soil depth whatever the treatment (M. Christina, G. Le Marie, P. Battie-Laclau, Y. Nouvellon, J.-P. Bouillet, C. Jourdan, J. L. de M. Goncalves, J.-P. Laclau, unpublished data).

Validation of the light interception submodel

The gap fractions were underestimated by 3% by the MAESPA model over the study period for all treatments (Fig. 2). The intercepted light (averaged over the five rings and five dates) was underestimated by 5% in +K−W and by 6% in −K−W, whereas it was overestimated by about 3% in +K+W and by 5% in −K+W.

Effect of K deficiency and W deficit on the stand aPAR, GPP and LUE$_C$

The time series for the stand aPAR and GPP exhibited a similar seasonality in all treatments (Fig. 3). Over the first 2 years after planting, the mean daily values for aPAR, GPP and LUE$_C$ were about 0.91 MJ m^{-2} day^{-1} (19%), 1.56 gC m^{-2} day^{-1} (24%) and 0.08 gC MJ^{-1} (6%) lower in the least productive treatment (−K−W) than

Table 3 Values of the morphological, physiological and root parameters used in the simulations

Stand age	+K +W 1 year	2 years	3 years	−K +W 1 year	2 years	3 years	+K−W 1 year	2 years	3 years	−K−W 1 year	2 years	3 years
Throughfall exclusion (%)	0%	0%	0%	0%	0%	0%	37%	37%	37%	37%	37%	37%
Morphological parameters												
LAI	3.35	4.53	5.14	2.57	2.59	1.88	3.60	3.94	4.29	2.48	2.76	2.01
H	4.98	10.51	15.48	3.64	7.27	10.79	5.22	10.49	14.96	3.97	7.74	11.44
D_c	3.0	3.3	3.5	2.7	3.2	3.5	2.9	3.2	3.4	2.7	3.0	3.2
LIA	28.2	45.5	48.9	24.2	34.9	41.5	32.4	47.5	50	29.6	41.5	42.3
Physiological parameters												
J_{MAX}		142.8	166.3		108.3	130.5		142.1	124.5		121.1	116.4
V_{CMAX}		45.9	91.8		50.3	62.8		63.2	70.8		45.6	50.4
R_d		1.32	2.91		1.45	2.65		1.82	2.24		1.17	1.71
α			0.354			0.307			0.288			0.361
K_p		0.92	1.33		0.58	1.43		0.88	1.93		0.73	1.59
Root parameters												
RMD	297	388.6	898.5	197	253.9	695.8	185	427.1	960.4	141	278.4	597.7
RAD		0.394	0.513		0.372	0.458		0.349	0.525		0.349	0.450
SRL		26.73	19.82		33.11	20.48		29.53	18.45		29.49	21.22
θ_M			0.145			0.151			0.123			0.125

Description of the parameters and their units is given in Table 1. Blank spaces correspond to year without measurements; in that case, the value was assumed equal to the next value.

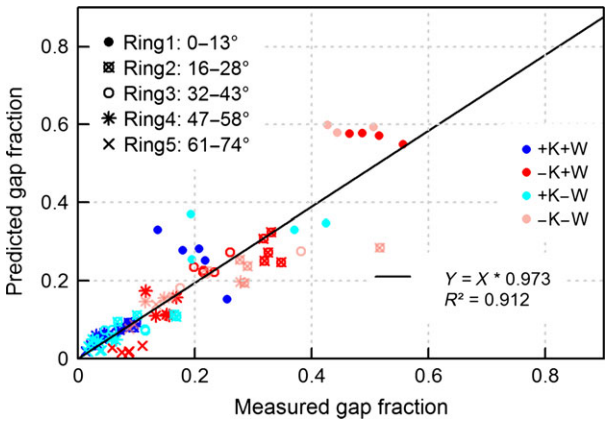

Fig. 2 Measured gap fractions compared with MAESPA simulations, on five dates between 2 and 3 years after planting. The line represents a linear regression between predicted (Y) and measured (X) values across all the rings, treatments and measurement dates.

in the most productive treatment (+K+W). The effects of the K and W supply regimes on aPAR, GPP and LUE_C sharply increased during the third year after planting. The mean annual values for aPAR, GPP and LUE_C were significantly higher in +K than in −K at all ages (Fig. 4). The third year after planting, throughfall exclusion did not reduce aPAR, but it was 21% lower in −K treatments than in +K treatments for both W supply regimes. Throughfall exclusion reduced GPP by 25% with +K treatments but had no significant affect with −K treatments. LUE_C ranged from 1.15 to 1.44 gC MJ^{-1} under various K and W supply regimes during the first 2 years after planting and increased by 22% in the third year in +K+W, whereas it remained unchanged in the other treatments.

The effect of K and W on Δ_{stem}, aPAR, GPP and LUE_C changed over the first 3 years after planting (Fig. 5). Throughfall exclusion led to 4–16% higher Δ_{stem}, aPAR, GPP and LUE_C in +K treatments the first year after planting but reduced Δ_{stem} by 25%, aPAR by 5%, GPP by 25% and LUE_C by 21% the third year after planting in −K treatments. −K+W and −K−W treatments reduced Δ_{stem}, aPAR, GPP and LUE_C over the whole study period (Δ_{stem} by 66%, aPAR by 21%, GPP by 31% and LUE_C by 13%, on average). There was an interaction between −K and −W treatments: the third year after planting, the reduction in GPP and LUE_C in −K−W was

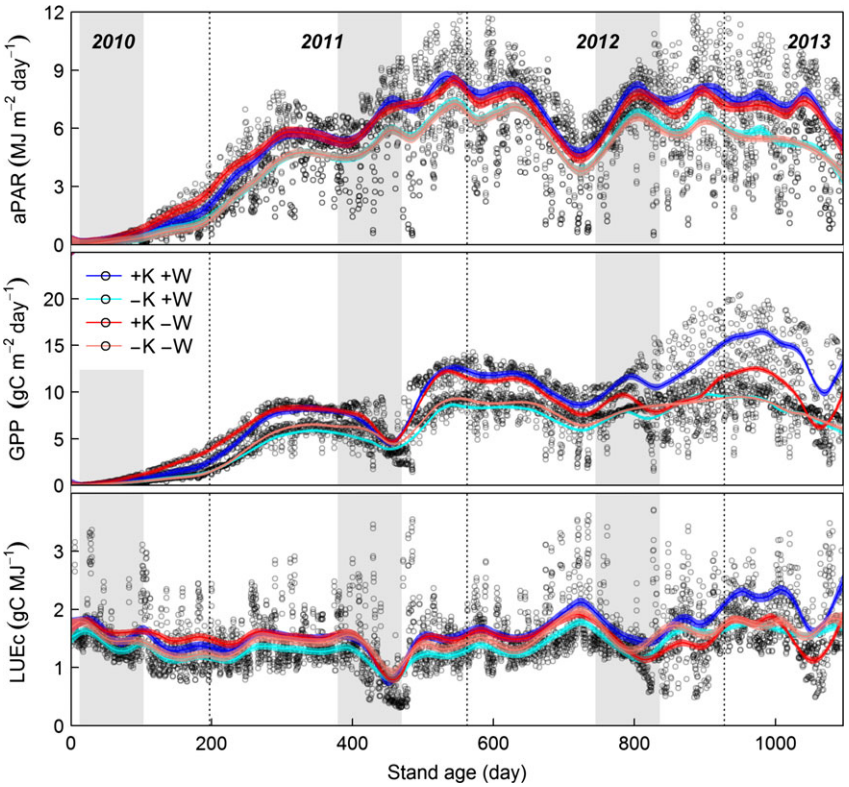

Fig. 3 Predicted daily-absorbed radiation (aPAR), gross photosynthesis (GPP) and light-use efficiency for carbon assimilation (LUE_C) of *Eucalyptus grandis* trees at stand scale, depending on potassium (K) and water (W) supply regimes. Black points are daily simulations for all treatments. For easier visual interpretation, the daily values of aPAR, GPP and LUE_C were fitted using smoothing splines (colored lines). Gray background areas show the dry seasons (from July to September).

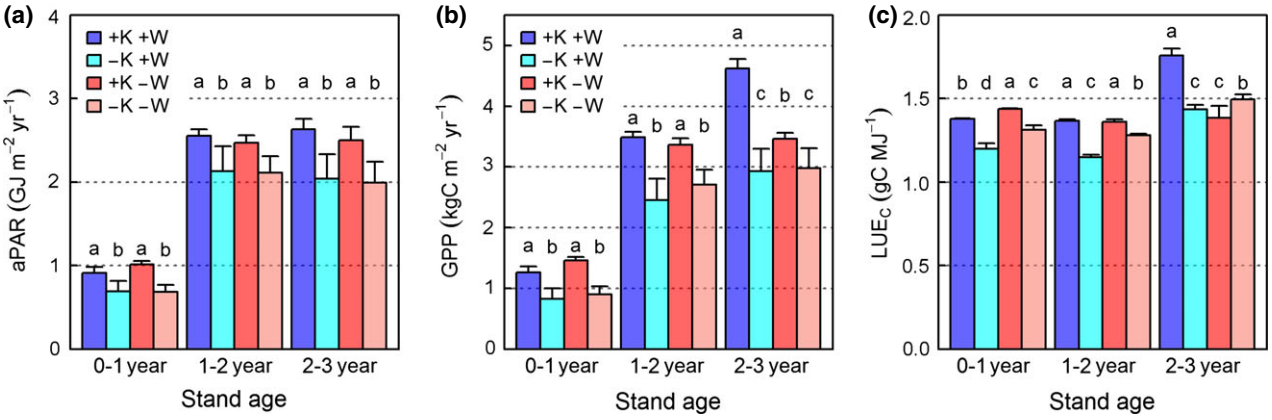

Fig. 4 Predicted annual absorbed radiation (aPAR, a), gross primary production (GPP, b) and light-use efficiency for carbon assimilation (LUE_C, c) at stand scale, depending on potassium (K) and water (W) supply regimes. Different letters at each age indicate significant differences between treatments ($P < 0.05$).

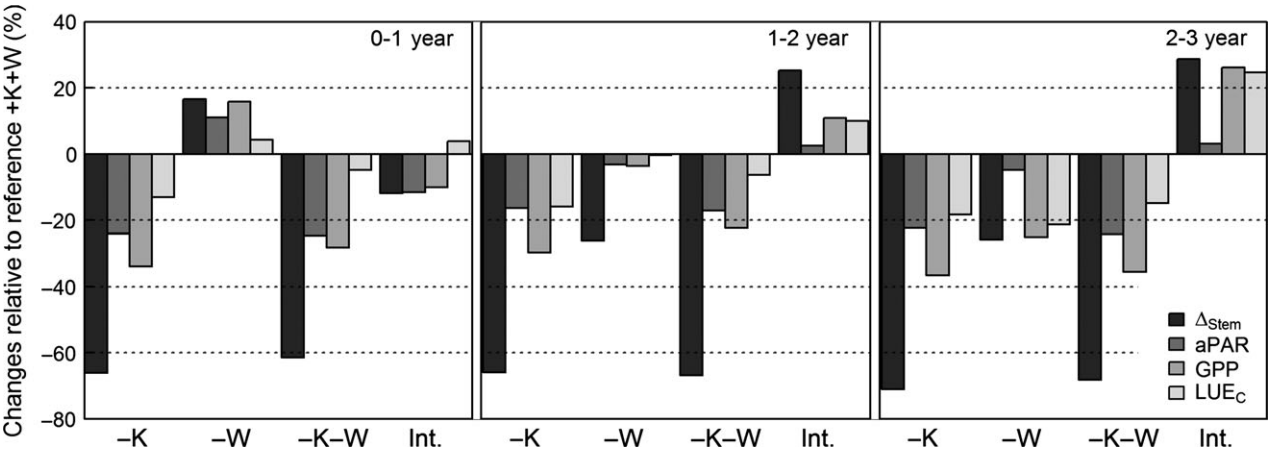

Fig. 5 Changes in stem biomass accumulation (Δ_{stem}), absorbed photosynthetic active radiation (aPAR), gross primary productivity (GPP) and light-use efficiency for carbon assimilation (LUE_C) relative to +K+W, in response to potassium deficiency (−K+W), water deficit (+K−W), combined effects of −K and −W (−K−W) and the interaction between −K and −W (Int.) in the 1st(left), 2nd(middle) and 3rd(right) year after planting.

about 25% less than the sum of the reductions caused by −K and −W individually.

Effect of tree height

Δ_{stem}, aPAR, GPP, $\%GPP_{stem}$ and LUE_S increased with tree height irrespective of the treatment over the first 2 years after planting (Fig. 6). In the third year, aPAR, GPP and Δ_{stem} were still positively correlated with tree height, but $\%GPP_{stem}$ and LUE_S were no longer affected by tree height for any treatment. At this age, $\%GPP_{stem}$ and LUE_S were 104% and 118% higher, respectively, in +K than in −K for both W supply regimes, and throughfall exclusion had no effect on $\%GPP_{stem}$ and LUE_S for either K supply regime. LUE_C was not related to tree height in the first 3 years after planting. The third year, LUE_C was 21% higher in +K+W than the other treatments.

Main factors driving aPAR, GPP and LUE_C

Simulations for the third year after planting, testing the whole set of tree parameters in +K+W by successively substituting each tree parameter measured in the other treatments (cf. eqn 6), made it possible to identify the main tree parameters responsible for the changes in the stand aPAR, GPP and LUE_C under K deficiency and W deficit (Figs 7 and 8).

aPAR was about 22% lower in −K than in +K, for all W supply regimes, mainly as a result of changes in LAI and tree height. K deficiency in +W reduced GPP by 37% and LUE_C by 18%, mainly in response to changes

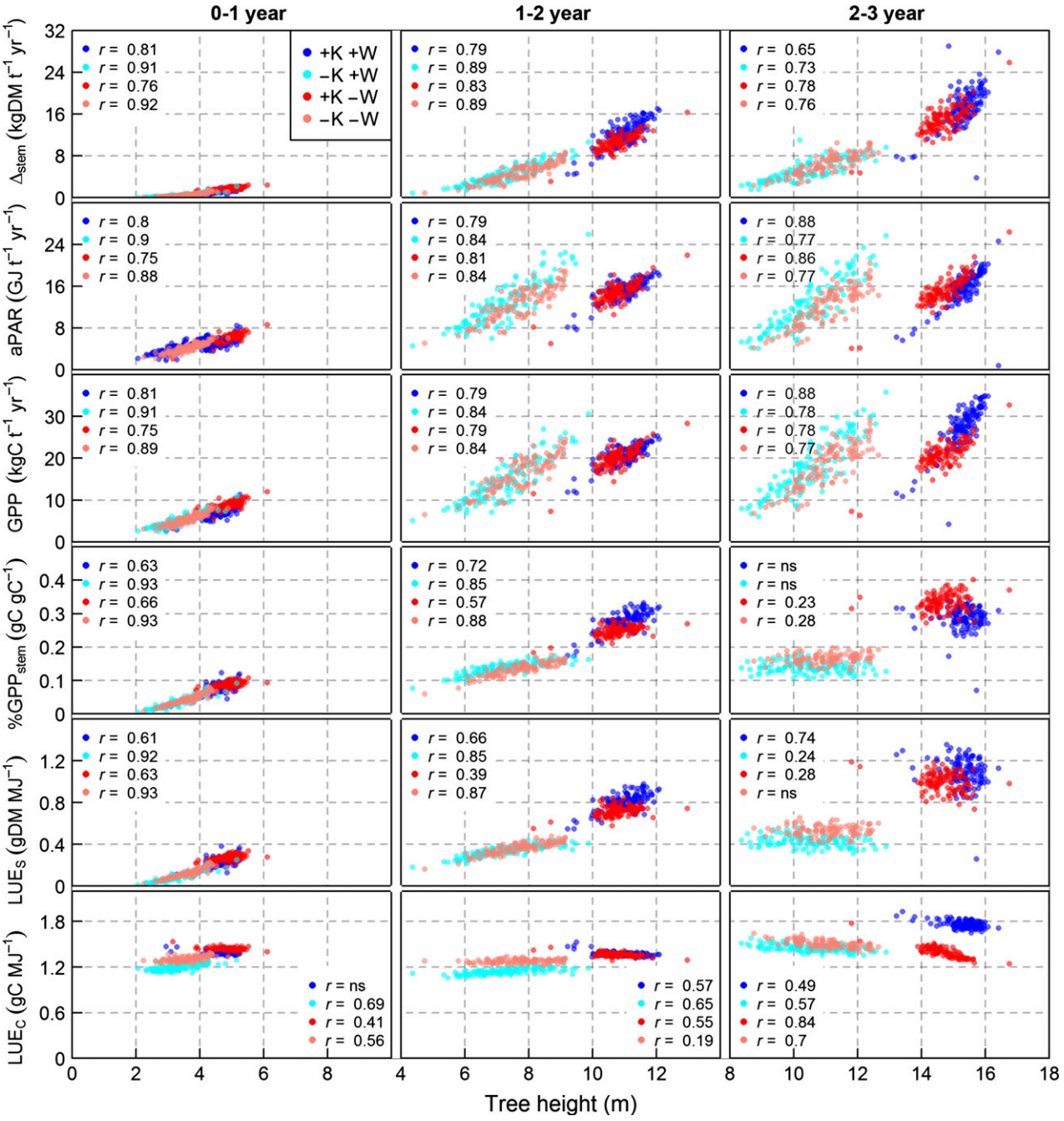

Fig. 6 Stem biomass accumulation (Δ_{stem}), absorbed PAR (aPAR), gross primary production (GPP), carbon allocated to stem production (%GPP_{stem}), light-use efficiency for stem biomass production (LUE_S) and light-use efficiency for carbon assimilation (LUE_C) in function of tree height for different potassium (K) and water (W) supplies, in the 1st (left column), 2nd (middle column) and year (right column) after planting. When significant at $P < 0.05$, correlation coefficients between the variables and tree height are shown by colors within each chart (ns: not significant at $P < 0.05$).

in minimum soil water content (θ_M), LAI, photosynthetic capacity (J_{MAX}, V_{CMAX}, α) and tree height, and, to a lesser extent, to soil-to-leaf hydraulic conductivity (K_p) and specific root length (SRL). K deficiency in −W decreased GPP by 14%, which was mainly the result of a lower LAI as well as changes in fine root distribution and, to a lesser extent, in θ_M. The effect of K deficiency on GPP was much less in −W than in +W as a result of a positive effect of α, K_p and fine root density in −K−W. LUE_C was 8% higher in −K−W as a result of the positive effects of the changes in H, α, K_p and SRL, on the one hand, and the negative effects of the changes in the

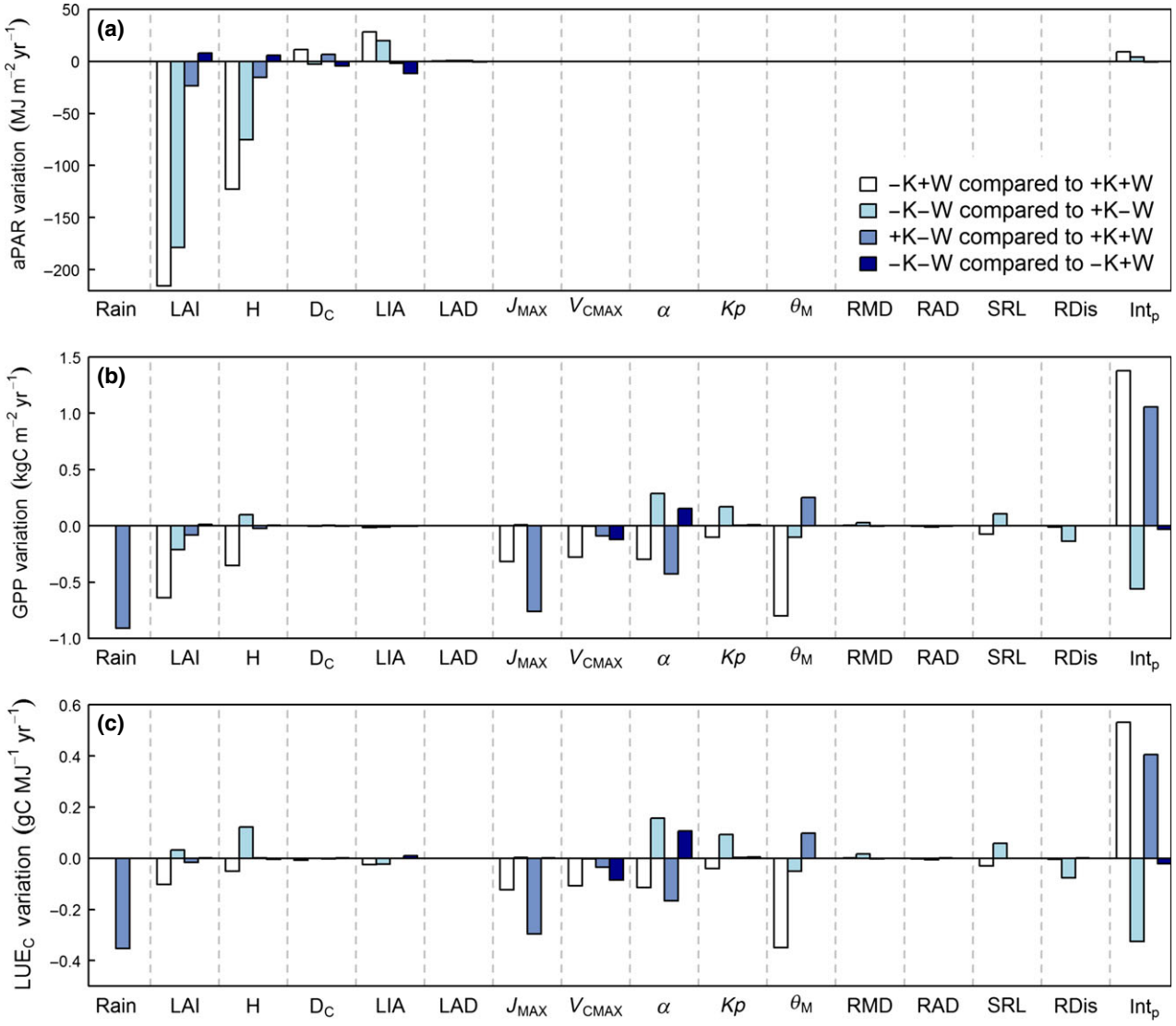

Fig. 7 Variations in aPAR (a), GPP (b) and LUE_C (c) due to the effect of each parameter, for a Eucalyptus plantation between 2 and 3 years after planting. Four effects are shown: K deficiency under undisturbed rainfall (−K+W compared to +K+W), K deficiency under throughfall exclusion (−K−W compared to +K−W), W deficit with adequate K supply (+K−W compared to +K+W) and W deficit for K-deficient trees (−K+W compared to −K−W). The tree parameters are described in Table 1. The '*Rain*' parameter refers to the amount of rainfall (undisturbed rainfall vs. 37% of throughfall exclusion for +W and −W, respectively). Int_p is the interaction between all parameters (see calculations in eqn 7). The annual values of aPAR, GPP and LUE_C are given in Fig. 4.

fine root distribution and θ_M on the other. Although the interaction between tree parameters (Int_p) had very little effect on aPAR, it had a greater effect on GPP and LUE_C than individual tree parameters.

For all K supply regimes, aPAR was 2–5% lower in −W than in +W the third year after planting and was little affected by the tree parameters tested in the model. Throughfall exclusion decreased GPP by 25% and decreased LUE_C by 21% for +K treatments. The main variables accounting for this pattern were the water supply regime (*Rain*), and the J_{MAX} and α parameters. With K deficiency, however, throughfall exclusion increased GPP slightly (by 2%) and LUE_C (by 4%), as a result of the opposite effects of αand V_{CMAX}.

Discussion

Simulations of aPAR, GPP and LUE

Simulated gap fractions were slightly underestimated compared to measured values. However, the discrepancies between measured and simulated gap fractions

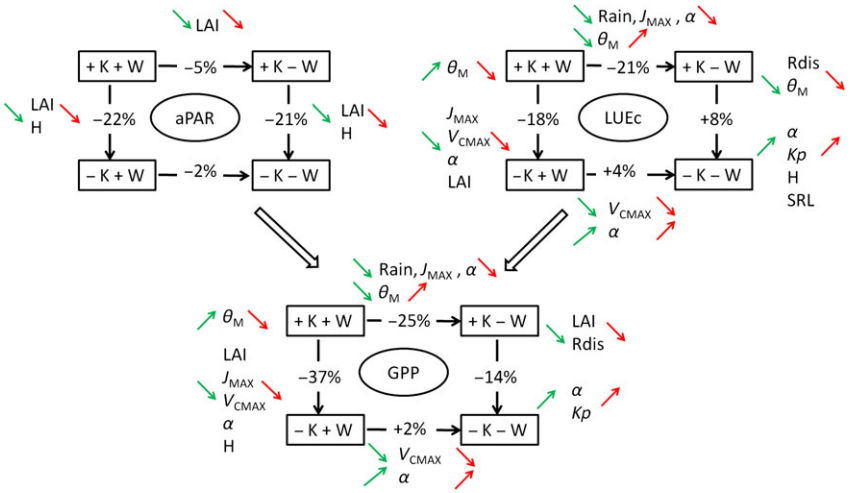

Fig. 8 Diagram of the main parameters affecting aPAR, GPP and LUE_C in response to K deficiency and water deficit (shown in Fig. 7), between 2 and 3 years after planting. Green arrows on the left of each parameter indicate whether the parameter increases or decreases. Red arrows on the right of each parameter indicate whether the parameter increases or decreases aPAR, GPP or LUE_C. The percentages of variation relative to mean annual values in Fig. 4 are shown. For instance, aPAR decreases by 5% with water reduction under normal K, and in that case, LAI is the only tree parameter which decreases enough to have a negative impact on aPAR.

were <6%, for all treatments, which was similar to other studies (Wang & Jarvis, 1990a; Bauerle *et al.*, 2004; Charbonnier *et al.*, 2013). aPAR predictions throughout tree growth in +K+W were of the same order of magnitude as in a nearby *E. grandis* plantation (Le Maire *et al.*, 2013).

The GPP values in our study were consistent with estimates based on measurements of aboveground net primary production and total belowground carbon flux between 5 and 7 years after planting in an adjacent experiment dealing with the response of *E. grandis* trees to K application (Epron *et al.*, 2012). The simulated GPP values for the third year after planting were 2.9 kgC m^{-2} yr^{-1} in −K+W and 4.6 kgC m^{-2} yr^{-1} in +K+W, close to the values estimated by Epron *et al.* (2012): GPP at 2.5 kgC m^{-2} yr^{-1} in −K plots and 4.4 kgC m^{-2} yr^{-1} in +K plots. GPP predictions obtained in our study from a detailed canopy structure parameterization and precise measurements of photosynthetic parameters within the crown (Fig. S1) were consistent with other estimates in Brazilian *Eucalyptus* plantations, which ranged from 2.9 to 4.2 kgC m^{-2} yr^{-1} in 3–6-year-old plantations, depending on the site and fertilization regime (Ryan *et al.*, 2010; Cabral *et al.*, 2011; Nouvellon *et al.*, 2012).

LUE_S increased from 0.23 gDM MJ^{-1} in the first year to about 1.1 gDM MJ^{-1} at 3 years for trees with added K, which was within the range of values reported for commercial *Eucalyptus* plantations (Whitehead & Beadle, 2004). LUE_S increased from about 0.3 gDM MJ^{-1} at 1 year to 1.2–1.6 gDM MJ^{-1} at 4 years in Brazilian *Eucalyptus* plantations (Stape *et al.*, 2004; Marsden *et al.*, 2010; Le Maire *et al.*, 2013). LUE_S ranged from 0.9 to 2.7 gDM MJ^{-1} at 6–9 years in Australian *E. globulus* plantations across a rainfall gradient (Landsberg & Hingston, 1996) and was estimated at 1.9 gDM MJ^{-1} at 1.5 years for Hawaiian *E. camaldulensis* plantations (Gower *et al.*, 1999).

Influence of tree nutrition and tree water status on LUE and GPP

The first hypothesis that K deficiency and rainfall deficit lead to a decrease in GPP as a result of a decrease in both aPAR and LUE_C was only valid after canopy closure. The first year after planting, LUE_C was little influenced by the K and W supply regimes and light absorption was the main driver of GPP. LAI values in K-deficient trees about half of those with an adequate supply of K have already been reported in *E. grandis* plantations (Laclau *et al.*, 2009; Epron *et al.*, 2012). aPAR and LUE_S were higher for big trees than for small trees at early growth stages, for all K and W supply regimes. Higher within-stand LUE_S for dominant trees relative to dominated trees is common in forest ecosystems but not systematic (Binkley *et al.*, 2010), and the lack of relationship between tree size and LUE_S after canopy closure in our study has already been reported for *E. grandis* plantations (Le Maire *et al.*, 2013). Efficiency in the use of captured resources to produce stem biomass usually increases with stand productivity (Giardina *et al.*, 2003; Binkley *et al.*, 2004; Stape *et al.*,

2004; Marsden *et al*., 2010). This pattern can be explained by a shift in C partitioning to produce stem biomass (shown by changes in $\%GPP_{stem}$) and/or an increase in LUE_C in response to an improvement in water and nutrient availability (Binkley *et al*., 2004). A shift of C partitioning to stem growth in response to K application was also observed at later growth stages in *E. grandis* trees (Epron *et al*., 2012).

High mobility of K^+ leads to intense recycling processes in forest ecosystems. The main fluxes of the K biogeochemical cycle were quantified over the development of eucalypt plantations in Congo and Brazil (Laclau *et al*., 2003, 2010). Foliar leaching returns K to the soil at about the same order of magnitude as the K content in the litter fall in eucalypt plantations. Potassium is released rapidly during litter decomposition and a fast uptake by eucalypt roots leads to the losses by deep drainage being less than the atmospheric inputs, even in sandy soils (Mareschal *et al*., 2013). In old tropical soils, the amounts of K released by weathering are negligible compared to K requirements for tree growth (Mareschal *et al*., 2011) and K fertilization is needed to sustain highly productive planted forests (Gonçalves *et al*., 2013). Many processes involved in C and K cycling depend on soil K availability in *E. grandis* plantations. K fertilization greatly increases leaf longevity (Laclau *et al*., 2010), individual leaf area (Battie-Laclau *et al*., 2013), K concentrations in the foliage (Battie-Laclau *et al*., 2014a) and in phloem sap (Battie-Laclau *et al*., 2014b), and K remobilization within stemwood (Sette *et al*., 2013). However, many field trials in tropical eucalypt plantations show strong interactions between N, P and K fertilizations for C and nutrient cycling (Gonçalves *et al*., 2013), as also shown by a fertilizer application experiment in a native tropical forest (Wright *et al*., 2011; Santiago *et al*., 2012). Previous studies showed that soil N and P availabilities limit tree growth the first year after planting at our study site (Laclau *et al*., 2009), even though K is the strongest limiting factor. Therefore, the effect of K deficiency on tree growth was higher in this experiment where large amounts of N and P have been added than in plantation when N, P and K together limit tree growth.

A strong effect of nutrient and water supply regimes on GPP is common in forest plantations. K application increased the GPP of 6-year-old *E. grandis* trees in Brazil by 75% (Epron *et al*., 2012). Although the K supply regime strongly influenced GPP from the first year after planting in our study, the effect of throughfall exclusion appeared only after canopy closure. This pattern was explained by the withdrawal of large amounts of water stored in deep soil layers after clear-cutting the previous stand (Nouvellon *et al*., 2014). Long-term throughfall exclusion experiments in forest ecosystems show that GPP and net primary production (NPP) are highly sensitive to rainfall distributions (Brando *et al*., 2008; Misson *et al*., 2010; Wu *et al*., 2011). Modeling approaches show that the response of forest NPP to rainfall reduction is highly site-dependent. For example, Luo *et al*. (2008) predicted that a decrease in precipitation by 50% in Northern Europe, USA and Brazil would decrease NPP in forest ecosystems by 10 to 50%. Cowling & Shin (2006) predicted that a decrease in precipitation by 50% would reduce NPP by 10–20% for a large part of the Amazon basin.

GPP and LUE_C under different W and K supply regimes: which are the most important tree parameters?

According to our second hypothesis, we identify the main tree parameters affected by K deficiency and throughfall exclusion, which were different for aPAR, LUE_C, and GPP. Although the treatments affected aPAR mainly through changes in LAI and tree height, changes in GPP and LUE were driven by a more complex set of parameters. Changes in photosynthetic capacity in response to K deficiency and throughfall exclusion had a considerable effect on GPP and LUE_C. Adding K increased the photosynthetic capacity (J_{MAX}, α), as shown by Pasquini & Santiago (2012). These results also suggest that a strong response of V_{CMAX} to K addition affected GPP and LUE_C in the +W treatments. A strong response of photosynthetic parameters to K availability has been shown for eucalypts (Battie-Laclau *et al*., 2014a), cotton (Gerardeaux *et al*., 2010), rice (Weng *et al*., 2007) and almond (Jin *et al*., 2011). A lower V_{CMAX} in K-deficient trees might also result from an accumulation of carbohydrates within K-deficient leaves (Battie-Laclau *et al*., 2014a), because K is needed for activation of starch synthase (Wakeel *et al*., 2011). Throughfall exclusion also led to a decrease in GPP and LUE_C by decreasing the capacity to convert light into chemical energy (J_{MAX}, α), which might be a result of dissipation of excitation energy through processes other than photosynthetic C-metabolism (Martinez-Ferri *et al*., 2000).

The trees were able to take up water down to lower soil water content in −W than in +W, and in +K than in −K, which strongly affected GPP. This behavior was represented in the model by the minimum soil water content parameter (θ_M). The treatment with the highest water demand (+K−W) had the lowest θ_M value indicating that the maximum amount of extractible water in the soil was greater than in the other treatments. This affects stomatal conductance (Tuzet model) and photosynthesis (Farquhar model) and, therefore, LUE. The capacity of plants to extract soil water depends on the fine root density, which is highly sensitive to nutrient

and water availability. Increased root growth in deep soil layers in response to water deficit is well documented (Dardanelli *et al*., 1997; Meier & Christoph, 2008; Cotrufo *et al*., 2011). Recent studies of *Arabidopsis* plants show that water potential gradients can control root growth, based on specific genes and plant hormones (Cassab *et al*., 2013). K deficiency has been shown to reduce fine root biomass in various plant species (Spollen *et al*., 1993; Egilla *et al*., 2001; Sangakkara *et al*., 2010), as well as in *E. grandis* plantations (Epron *et al*., 2012). Surprisingly, the fine root biomass parameter (RMD) had a weak effect on GPP predictions in our simulations, probably because root biomass was only used in the model in the soil-to-root resistance calculation, which does not appear as a major limiting factor. Nevertheless, fine root biomass also influences GPP and LUE by modifying θ_M. Similarly, large differences in R_{dis} and specific root length between treatments had a low effect on GPP and LUE_C. The low sensibility of such parameter might be explained by the plasticity of fine root growth in response to environmental constraints (Zhang *et al*., 2009) which may be sufficient to supply the soil resources needed to reach GPP and LUE_C. Stand GPP and LUE_C may be limited by nonoptimal root distributions only under very limiting K and W conditions (−K−W).

Interaction between K and W supply regimes on GPP and LUE_C

In agreement with our third hypothesis, there was a strong interaction between K and W supply regimes, which affected the measured stem biomass production, as well as the simulated LUE and GPP. The effect on aPAR, however, was negligible, mainly because throughfall exclusion had a very little effect on aPAR.

One of the main objectives of process-based models is to simulate interactions to make the modeling of 'elementary' processes more realistic. A possible source of interactions in the model is the presence of intrinsic interactions in the input parameters. For instance, the LAI parameter was reduced by 25% in response to throughfall exclusion (+K−W), 66% in response to K deficiency (−K+W) and only 64% in response to both K deficiency and throughfall exclusion (−K−W). Another source of interactions in the model, which adds to the input parameter interactions, is the nonlinear response of various processes to the values of the parameters. The model outputs can be more or less sensitive to a parameter depending on its range of values or the values of other parameters. Threshold responses, which are common in process-based models, have similar effects. Interactions can also come from new processes not taken into account when K deficiency and water deficit are simulated separately. Although these new processes should be included in the model to simulate these interactions correctly, they are often difficult to identify. Comprehensive field studies measuring most of the input parameters used in ecophysiological models are, therefore, needed to improve the prediction of the effects of nutrient deficiency and water deficit.

In our experiment, the effect of combined K deficiency and throughfall exclusion on stem biomass production and GPP was close to the effect of K deficiency alone, despite a strong effect of throughfall exclusion on its own. Although tree growth was mainly limited by K availability before canopy closure as a result of the withdrawal of large amounts of water stored in deep soil layers (Battie-Laclau *et al*., 2014b), tree growth was limited subsequently by both K and water availability. Battie-Laclau *et al*. (2014b) showed in the same experiment that water stress during dry periods was higher for K-fertilized trees than for K-deficient trees as a result of higher LAI and water demand. The interaction between K and W deficiencies reflected, therefore, a much higher effect of throughfall exclusion for K-fertilized trees than for K-deficient trees. Many processes influence the interaction between K and W supply regimes on stem biomass production and GPP through carbon and water cycling. For example, it appears that lower J_{MAX} in −K than in +K does not influence GPP under throughfall exclusion (comparing −K−W to +K−W), whereas it was a major cause of lower GPP in −K+W relative to +K+W.

Consequences for forest management in drought prone regions

Few throughfall exclusion experiments have been undertaken in planted forests to investigate the interactions between nutrient deficiency and water deficit (Wu *et al*., 2011; Battie-Laclau *et al*., 2014b). A growing body of evidence suggests that trees are less prone to water deficit in infertile soils than under high nutrient availability as was shown by the low effect of throughfall exclusion on tree morphology and physiology in the −K treatments. A similar effect has been shown for grassland species (Zhang, 1996) and desert plants (Zhou *et al*., 2011). Nutrient (particularly K) availability is a key factor influencing tree water loss (through changes in leaf area, osmotic adjustment, stomatal regulation, etc). Moreover, fast-growing species with high stomatal conductance, such as *E. grandis*, maintain high photosynthesis rates throughout drought periods, making it possible to avoid death through C starvation during extreme drought (McDowell *et al*., 2008). Nonetheless, a consequence of such a strategy is possible death through hydraulic fail-

ure (Mitchell *et al*., 2013). Management practices decreasing the water demand in planted forests can help to prevent tree mortality in a future drier climate (White *et al*., 2009, 2014). A reduction of stocking densities or a decrease in fertilizer doses relative to current silvicultural practices would reduce stand water use and, therefore, the risk of tree mortality during extreme droughts. This would, however, reduce the yield in these planted forests.

As a conclusion, the decrease in GPP in response to K deficiency and water deficit resulted from a decrease in aPAR during the early growth stages and a decrease in both aPAR and LUE after canopy closure. This modeling approach revealed that leaf photosynthetical parameters, the tree parameters governing soil water uptake and interactions between these parameters were the main drivers of the GPP and LUE responses to K deficiency and W deficit. The substantial changes in the use of light and C in *E. grandis* trees which occur with K addition suggest that key biochemical mechanisms involved in K cycling should be taken into account in process-based models designed to predict the net primary productivity of forests on K-deficient soils. This study also suggests that, in a context of climate change, recommended levels of nutrient supply in planted forests should be revised to improve tree tolerance to severe drought.

Acknowledgements

The study was funded by Universidade de São Paulo, Centre de coopération Internationale en Recherche Agronomique pour le Développement (CIRAD), SOERE F-ORE-T, and Agence Nationale de la Recherche (Maccac project, AGROBIOSPHERE program). This work has benefited from the support of Agropolis Foundation as part of the program 'Investissements d'avenir' (ANR-10-LabX-0001-01) and from the support of the Brazilian state of 'Programa de Cooperação internacional capes/ Fundação AGROPOLIS 017/2013'. We are grateful to the staff at the Itatinga Experimental Station, in particular Rildo Moreira e Moreira (Esalq, USP), as well as Eder Araújo da Silva (http://www.floragroapoio.com.br) for their technical support. We are grateful to Tony Tebby for correcting the English language.

References

Almeida AC, Siggins A, Batista TR, Beadle C, Fonseca S, Loos R (2010) Mapping the effect of spatial and temporal variation in climate and soils on Eucalyptus plantation production with 3-PG, a process-based growth model. *Forest Ecology and Management*, **259**, 1730–1740.

Battie-Laclau P, Laclau J-P, de Cassia Piccolo M *et al*. (2013) Influence of potassium and sodium nutrition on leaf area components in *Eucalyptus grandis* trees. *Plant and Soil*, **371**, 19–35.

Battie-Laclau P, Laclau J-P, Beri C *et al*. (2014a) Photosynthetic and anatomical responses of *Eucalyptus grandis* leaves to potassium and sodium supply in a field experiment. *Plant, Cell & Environment*, **37**, 70–81.

Battie-Laclau P, Laclau J-P, Domec J-C *et al*. (2014b) Effects of potassium and sodium supply on drought-adaptive mechanisms in *Eucalyptus grandis* plantations. *The New Phytologist*, **203**, 401–413.

Bauerle WL, Bowden JD, McLeod MF, Toler JE (2004) Modeling intra-crown and intra-canopy interactions in red maple: assessment of light transfer on carbon dioxide and water vapor exchange. *Tree Physiology*, **24**, 589–597.

Binkley D, Stape JL, Ryan MG (2004) Thinking about efficiency of resource use in forests. *Forest Ecology and Management*, **193**, 5–16.

Binkley D, Stape JL, Bauerle WL, Ryan MG (2010) Explaining growth of individual trees: light interception and efficiency of light use by Eucalyptus at four sites in Brazil. *Forest Ecology and Management*, **259**, 1704–1713.

Binkley D, Laclau JP, Sterba H (2013) Why one tree grows faster than another: patterns of light use and light use efficiency at the scale of individual trees and stands. *Forest Ecology and Management*, **288**, 1–4.

Booth TH (2013) Eucalypt plantations and climate change. *Forest Ecology and Management*, **301**, 28–34.

Brando PM, Nepstad DC, Davidson EA, Trumbore SE, Ray D, Camargo P (2008) Drought effects on litterfall, wood production and belowground carbon cycling in an Amazon forest: results of a throughfall reduction experiment. *Philosophical Transactions of the Royal Society B-Biological Sciences*, **363**, 1839–1848.

Cabral OMR, Gash JHC, Rocha HR *et al*. (2011) Fluxes of CO2 above a plantation of Eucalyptus in southeast Brazil. *Agricultural and Forest Meteorology*, **151**, 49–59.

Cakmak I (2005) The role of potassium in alleviating detrimental effects of abiotic stresses in plants. *Journal of Plant Nutrition and Soil Science*, **168**, 521–530.

Cakmak I, Hengeler C, Marschner H (1994) Changes in phloem export of sucrose in leaves in response to phosphorus, potassium and magnesium deficiency in bean plants. *Journal of Experimental Botany*, **45**, 1251–1257.

Carter JL, White DA (2009) Plasticity in the Huber value contributes to homeostasis in leaf water relations of a mallee Eucalypt with variation to groundwater depth. *Tree Physiology*, **29**, 1407–1418.

Cassab GI, Eapen D, Campos ME (2013) Root hydrotropism: an update. *American Journal of Botany*, **100**, 14–24.

Charbonnier F, le Maire G, Dreyer E *et al*. (2013) Competition for light in heterogeneous canopies: application of MAESTRA to a coffee (*Coffea arabica* L.) agroforestry system. *Agricultural and Forest Meteorology*, **181**, 152–169.

Christina M, Laclau JP, Gonçalves JLM, Jourdan C, Nouvellon Y, Bouillet JP (2011) Almost symmetrical vertical growth rates above and below ground in one of the world's most productive forests. *Ecosphere*, **2**, 1–10.

Cochrane TT, Cochrane TA (2009) Differences in the way potassium chloride and sucrose solutions effect osmotic potential of significance to stomata aperture modulation. *Plant Physiology and Biochemistry: PPB/Société Française de Physiologie Végétale*, **47**, 205–209.

Cotrufo MF, Alberti G, Inglima I *et al*. (2011) Decreased summer drought affects plant productivity and soil carbon dynamics in a Mediterranean woodland. *Biogeosciences*, **8**, 2729–2739.

Cowling SA, Shin Y (2006) Simulated ecosystem threshold responses to co-varying temperature, precipitation and atmospheric CO 2 within a region of Amazonia. *Global Ecology and Biogeography*, **15**, 553–566.

Dardanelli JL, Bachmeier OA, Sereno R, Gil R (1997) Rooting depth and soil water extraction patterns of different crops in a silty loam Haplustoll. *Field Crops Research*, **54**, 29–38.

Darunsontaya T, Suddhiprakarn A, Kheoruenromne I, Prakongkep N, Gilkes RJ (2012) The forms and availability to plants of soil potassium as related to mineralogy for upland Oxisols and Ultisols from Thailand. *Geoderma*, **170**, 11–24.

Duursma RA, Medlyn B (2012) MAESPA: a model to study interactions between water limitation, environmental drivers and vegetation function at tree and stand levels, with an example application to [CO2] × drought interactions. *Geoscientific Model Development Discussions*, **5**, 919–940.

Egilla JN, Davies FT, Drew MC (2001) Effect of potassium on drought resistance of Hibiscus rosa-sinensis cv. Leprechaun: plant growth, leaf macro- and micronutrient content and root longevity. *Plant and Soil*, **229**, 213–224.

Epron D, Laclau JP, Almeida JCR *et al*. (2012) Do changes in carbon allocation account for the growth response to potassium and sodium applications in tropical Eucalyptus plantations? *Tree Physiology*, **32**, 667–679.

Farquhar GD, von Caemmerer S, Berry JA (1980) A biochemical model of photosynthetic CO2 assimilation in leaves of C3 species. *Planta*, **149**, 78–90.

Food and Agriculture Organization of the United Nations (2011) *State of the World 's Forest*. FAO, Rome.

Gajdanowicz P, Michard E, Sandmann M *et al*. (2011) Potassium (K+) gradients serve as a mobile energy source in plant vascular tissues. *Proceedings of the National Academy of Sciences of the United States of America*, **108**, 864–869.

Gerardeaux E, Jordan-Meille L, Constantin J, Pellerin S, Dingkuhn M (2010) Changes in plant morphology and dry matter partitioning caused by potassium deficiency in *Gossypium hirsutum* (L.). *Environmental and Experimental Botany*, **67**, 451–459.

Giardina CP, Ryan MG, Binkley D, Fownes JH (2003) Primary production and carbon allocation in relation to nutrient supply in a tropical experimental forest. *Global Change Biology*, **9**, 1438–1450.

Gonçalves JLDM, Alvares CA, Higa AR *et al.* (2013) Integrating genetic and silvicultural strategies to minimize abiotic and biotic constraints in Brazilian eucalypt plantations. *Forest Ecology and Management*, **301**, 6–27.

Gower ST, Kucharik CJ, Norman JM (1999) Direct and indirect estimation of leaf area index, fAPAR, and net primary production of terrestrial ecosystems. *Remote Sensing of Environment*, **70**, 29–51.

Hilker T, Coops NC, Wulder MA, Black TA, Guy RD (2008) The use of remote sensing in light use efficiency based models of gross primary production: a review of current status and future requirements. *The Science of the Total Environment*, **404**, 411–423.

IPCC (2013) Summary for policymakers. In: *Climate Change 2013: The Physical Science Basis. Contribution of Working Group I to the Fifth Assessment Report of the Intergovernmental Panel on Climate Change* (eds Stocker TF, Qin D, Plattner GK, Tignor MMB, Allen SK, Boschung J, Nauels A, Xia Y, Bex V, Midgley PM), pp. 1–30. Cambridge University Press, Cambridge.

Jin SH, Huang JQ, Li XQ *et al.* (2011) Effects of potassium supply on limitations of photosynthesis by mesophyll diffusion conductance in *Carya cathayensis*. *Tree Physiology*, **31**, 1142–1151.

Kim YJ, Gu C (2004) Smoothing spline Gaussian regression: more scalable computation via efficient approximation. *Journal of the Royal Statistical Society Series B-Statistical Methodology*, **66**, 337–356.

Kreuzwieser J, Gessler A (2010) Global climate change and tree nutrition: influence of water availability. *Tree Physiology*, **30**, 1221–1234.

Laclau J-P, Deleporte P, Ranger J, Bouillet J-P, Kazotti G (2003) Nutrient dynamics throughout the rotation of Eucalyptus clonal stands in Congo. *Annals of Botany*, **91**, 879–892.

Laclau J-P, Almeida JCR, Gonçalves JLM *et al.* (2009) Influence of nitrogen and potassium fertilization on leaf lifespan and allocation of above-ground growth in Eucalyptus plantations. *Tree Physiology*, **29**, 111–124.

Laclau JP, Ranger J, de Moraes Gonçalves JL *et al.* (2010) Biogeochemical cycles of nutrients in tropical Eucalyptus plantations. Main features shown by intensive monitoring in Congo and Brazil. *Forest Ecology and Management*, **259**, 1771–1785.

Landsberg J, Hingston F (1996) Evaluating a simple radiation/dry matter conversion model using data from Eucalyptus globulus plantations in Western Australia. *Tree Physiology*, **16**, 801–808.

Le Maire G, Nouvellon Y, Christina M, Ponzoni FJ, Gonçalves JLM, Bouillet JP, Laclau JP (2013) Tree and stand light use efficiencies over a full rotation of single-and mixed-species *Eucalyptus grandis* and *Acacia mangium* plantations. *Forest Ecology and Management*, **288**, 31–42.

Luo Y, Gerten D, Le Maire G *et al.* (2008) Modeled interactive effects of precipitation, temperature, and CO2 on ecosystem carbon and water dynamics in different climatic zones. *Global Change Biology*, **14**, 1986–1999.

Maquere V (2008) *Dynamique des éléments minéraux sous plantation intensive d'Eucalyptus au Brésil*. Conséquences pour la durabilité des sols. PhD thesis. AgroParisTech, France. Available at: https://pastel.archives-ouvertes.fr/pastel-00610330 (accessed 1 September 2014).

Mareschal L, Nzila JDD, Turpault MP *et al.* (2011) Mineralogical and physico-chemical properties of Ferralic Arenosols derived from unconsolidated Plio-Pleistocenic deposits in the coastal plains of Congo. *Geoderma*, **162**, 159–170.

Mareschal L, Laclau J-P, Nzila J-D-D *et al.* (2013) Nutrient leaching and deep drainage under Eucalyptus plantations managed in short rotations after afforestation of an African savanna: two 7-year time series. *Forest Ecology and Management*, **307**, 242–254.

Marsden C, le Maire G, Stape J-L *et al.* (2010) Relating MODIS vegetation index time-series with structure, light absorption and stem production of fast-growing Eucalyptus plantations. *Forest Ecology and Management*, **259**, 1741–1753.

Martinez-Ferri E, Balaguer L, Valladares F, Chico JM, Manrique E (2000) Energy dissipation in drought-avoiding and drought-tolerant tree species at midday during the Mediterranean summer. *Tree Physiology*, **20**, 131–138.

McDowell N, Pockman WT, Allen CD *et al.* (2008) Mechanisms of plant survival and mortality during drought: why do some plants survive while others succumb to drought? *The New Phytologist*, **178**, 719–739.

Medlyn BE (1998) Physiological basis of the light use efficiency model. *Tree Physiology*, **18**, 167–176.

Medlyn BE, Dreyer E, Ellsworth D *et al.* (2002) Temperature response of parameters of a biochemically based model of photosynthesis. II. A review of experimental data. *Plant, Cell and Environment*, **25**, 1167–1179.

Medlyn BE, Pepper DA, O'Grady AP, Keith H (2007) Linking leaf and tree water use with an individual-tree model. *Tree Physiology*, **27**, 1687–1699.

Meier IC, Christoph L (2008) Belowground drought response of European beech: fine root biomass and carbon partitioning in 14 mature stands across a precipitation gradient. *Global Change Biology*, **14**, 2081–2095.

Mengel K, Arneke WW (1982) Effect of potassium on the water potential, the pressure potential, the osmotic potential and cell elongation in leaves of *Phaseolus vulgaris*. *Physiologia Plantarum*, **54**, 402–408.

Miao Z, Xu M, Lathrop RG, Wang Y (2009) Comparison of the A-Cc curve fitting methods in determining maximum ribulose 1.5-bisphosphate carboxylase/oxygenase carboxylation rate, potential light saturated electron transport rate and leaf dark respiration. *Plant, Cell & Environment*, **32**, 109–122.

Misson L, Rocheteau A, Rambal S, Ourcival JM, Limousin JM, Rodriguez R (2010) Functional changes in the control of carbon fluxes after 3 years of increased drought in a Mediterranean evergreen forest? *Global Change Biology*, **16**, 2461–2475.

Mitchell PJ, O'Grady AP, Tissue DT, White DA, Ottenschlaeger ML, Pinkard EA (2013) Drought response strategies define the relative contributions of hydraulic dysfunction and carbohydrate depletion during tree mortality. *New Phytologist*, **197**, 862–872.

Nelder JA, Mead R (1965) A simplex method for function minimization. *Computer Journal*, **7**, 308–313.

Norman JM, Welles JM (1983) Radiative transfer in an array of canopies. *Agronomy Journal*, **75**, 481–488.

Nouvellon Y, Laclau JP, Epron D, Le Maire G, Bonnefond JM, Goncalves JLM, Bouillet JP (2012) Production and carbon allocation in monocultures and mixed-species plantations of *Eucalyptus grandis* and *Acacia mangium* in Brazil. *Tree Physiology*, **32**, 680–695.

Nouvellon Y, Stape JL, Bonnefond JM *et al.* (2014). Carbon, water and nutrient balances of an *Eucalyptus grandis* plantation in Brazil over a 5 yrs period. IUFRO World Congress 2014, Oct 5-11, Salt Lake City, (oral presentation).

Paquette A, Messier C (2010) The role of plantations in managing the world's forests in the Anthropocene. *Frontiers in Ecology and the Environment*, **8**, 27–34.

Pasquini SC, Santiago LS (2012) Nutrients limit photosynthesis in seedlings of a lowland tropical forest tree species. *Oecologia*, **168**, 311–319.

Peñuelas J, Poulter B, Sardans J *et al.* (2013) Human-induced nitrogen-phosphorus imbalances alter natural and managed ecosystems across the globe. *Nature Communications*, **4**, 2934.

Piao S, Sitch S, Ciais P *et al.* (2013) Evaluation of terrestrial carbon cycle models for their response to climate variability and to CO2 trends. *Global Change Biology*, **19**, 2117–2132.

R Development Core Team (2014) *R: A Language and Environment for Statistical Computing*. R Development Core Team, Vienna.

Reddy AR, Chaitanya KV, Vivekanandan M (2004) Drought-induced responses of photosynthesis and antioxidant metabolism in higher plants. *Journal of Plant Physiology*, **161**, 1189–1202.

Römheld V, Kirkby EA (2010) Research on potassium in agriculture: needs and prospects. *Plant and Soil*, **335**, 155–180.

Ryan MG, Stape JL, Binkley D *et al.* (2010) Factors controlling Eucalyptus productivity: how water availability and stand structure alter production and carbon allocation. *Forest Ecology and Management*, **259**, 1695–1703.

Sangakkara UR, Amarasekera P, Stamp P (2010) Irrigation regimes affect early root development, shoot growth and yields of maize (*Zea mays* L.) in tropical minor seasons. *Plant Soil and Environment*, **56**, 228–234.

Santiago LS, Wright SJ, Harms KE, Yavitt JB, Korine C, Garcia MN, Turner BL (2012) Tropical tree seedling growth responses to nitrogen, phosphorus and potassium addition. *Journal of Ecology*, **100**, 309–316.

Seager R, Ting M, Held I *et al.* (2007) Model projections of an imminent transition to a more arid climate in southwestern North America. *Science*, **316**, 1181–1184.

Sette CR, Laclau J-P, Tomazello Filho M, Moreira RM, Bouillet J-P, Ranger J, Almeida JCR (2013) Source-driven remobilizations of nutrients within stem wood in *Eucalyptus grandis* plantations. *Trees*, **27**, 827–839.

Sheffield J, Wood EF (2008) Projected changes in drought occurrence under future global warming from multi-model, multi-scenario, IPCC AR4 simulations. *Climate Dynamics*, **31**, 79–105.

Sjöström M, Zhao M, Archibald S *et al.* (2013) Evaluation of MODIS gross primary productivity for Africa using eddy covariance data. *Remote Sensing of Environment*, **131**, 275–286.

Smethurst PJ (2010) Forest fertilization: trends in knowledge and practice compared to agriculture. *Plant and Soil*, **335**, 83–100.

Spollen E.G., Sharp R.E., Saab I.N., Wu Y (1993) Regulation of cell expansion in roots and shoots at low water potentials. In: *Water Deficits: Plant Responses From Cell to Community* (ed. Press O), pp. 37–52. BIOS Scientific Publishers Ltd., Oxford.

Stape JL, Binkley D, Ryan MG (2004) Eucalyptus production and the supply, use and efficiency of use of water, light and nitrogen across a geographic gradient in Brazil. *Forest Ecology and Management*, **193**, 17–31.

Tuzet A, Perrier A, Leuning R (2003) A coupled model of stomatal conductance, photosynthesis and transpiration. *Plant, Cell & Environment*, **26**, 1097–1116.

Van Genuchten MT (1980) A closed-form equation for predicting the hydraulic conductivity of unsaturated soils. *Soil Science Society of America Journal*, **44**, 892–898.

Wakeel A, Farooq M, Qadir M, Schubert S (2011) Potassium substitution by sodium in plants. *Critical Reviews in Plant Sciences*, **30**, 401–413.

Wang YP, Jarvis PG (1990a) Description and validation of an array model–MAESTRO. *Agricultural and Forest Meteorology*, **51**, 257–280.

Wang YP, Jarvis PG (1990b) Influence of crown structural properties on PAR absorption, photosynthesis, and transpiration in Sitka spruce: application of a model (MAESTRO). *Tree Physiology*, **7**, 297–316.

Wang M, Zheng Q, Shen Q, Guo S (2013) The critical role of potassium in plant stress response. *International Journal of Molecular Sciences*, **14**, 7370–7390.

Weng XY, Zheng CJ, Xu HX, Sun JY (2007) Characteristics of photosynthesis and functions of the water-water cycle in rice (*Oryza sativa*) leaves in response to potassium deficiency. *Physiologia Plantarum*, **131**, 614–621.

White DA, Crombie DS, Kinal J, Battaglia M, McGrath JF, Mendharn DS, Walker SN (2009) Managing productivity and drought risk in Eucalyptus globulus plantations in south-western Australia. *Forest Ecology and Management*, **259**, 33–44.

White DA, McGrath JF, Ryan MG *et al.* (2014) Managing for water-use efficient wood production in Eucalyptus globulus plantations. *Forest Ecology and Management*, **331**, 272–280.

Whitehead D, Beadle CL (2004) Physiological regulation of productivity and water use in Eucalyptus: a review. *Forest Ecology and Management*, **193**, 113–140.

Williams M, Bond BJ, Ryan MG (2001a) Evaluating different soil and plant hydraulic constraints on tree function using a model and sap flow data from ponderosa pine. *Plant, Cell and Environment*, **24**, 679–690.

Williams M, Law BE, Anthoni PM, Unsworth MH (2001b) Use of a simulation model and ecosystem flux data to examine carbon–water interactions in ponderosa pine. *Tree Physiology*, **21**, 287–298.

Wright SJ, Yavitt JB, Wurzburger N *et al.* (2011) Potassium, phosphorus, or nitrogen limit root allocation, tree growth, or litter production in a lowland tropical forest. *Ecology*, **92**, 1616–1625.

Wu ZT, Dijkstra P, Koch GW, Penuelas J, Hungate BA (2011) Responses of terrestrial ecosystems to temperature and precipitation change: a meta-analysis of experimental manipulation. *Global Change Biology*, **17**, 927–942.

Yang F, Ichii K, White MA *et al.* (2007) Developing a continental-scale measure of gross primary production by combining MODIS and AmeriFlux data through Support Vector Machine approach. *Remote Sensing of Environment*, **110**, 109–122.

Zhang JH (1996) Interactive effects of soil nutrients, moisture and sand burial on the development, physiology, biomass and fitness of *Cakile edentula*. *Annals of Botany*, **78**, 591–598.

Zhang Y, Zhou Z, Ma X, Jin G (2009) Foraging ability and growth performance of four subtropical tree species in response to heterogeneous nutrient environments. *Journal of Forest Research*, **15**, 91–98.

Zhou XB, Zhang YM, Ji XH, Downing A, Serpe M (2011) Combined effects of nitrogen deposition and water stress on growth and physiological responses of two annual desert plants in northwestern China. *Environmental and Experimental Botany*, **74**, 1–8.

Supporting Information

Additional Supporting Information may be found in the online version of this article:

Figure S1. A–Ci curves used in the model, with different water (W) and potassium (K) availabilities.
Table S1. Average and standard deviation on photosynthetical parameters (J_{MAX}, V_{CMAX}, R_d) depending of treatments, tree ages and position within the crown (Inf = inferior, Med = medium and Sup = Superior).
Table S2. Multiple regression of the effect of water (W), potassium (K) and tree age on the stomatal conductance response to photosynthesis (Gs), and vertical (VLAD) and horizontal leaf area densities (HLAD).